GIS and DEM Based Watershed Characteristics of Wadi Al-Adaira Basin, KSA

Wafaa S. Al-Khuraiji∗
Fahda F. Ben-Hasher∗
Ali A. Aldosari∗∗
Mohamed S. Al-Farhan∗∗∗

ABSTRACT

The study aimed to evaluate the possibility of using the digital elevation model (DEM) technique based on GIS in the automatic extraction of the drainage basin network and calculating its parameters. The study used the digital elevation model from ASTER DEM (30 m) data for Wadi Al-Adaira basin and its sub-basins using Arc GIS 10.5 and its extensions: spatial analyst tools, 3D analyst tools and ArcHydro and then computed the morphometric parameters for the drainage of sub basins. Morphometric parameters for drainage basins include: Area (ranged between 92.5 km^2 and 3323.06 km^2), Max. Length (ranged between 17.06 km and 152.93 km), average width (ranged between 4.51 km and 21.73 km), perimeter (ranged between 62.45 km and 610.03 km), elongation ratio (ranged between 0.43 and 0.77), circulation ratio (ranged between 0.11 and 0.32), and form factor (ranged between 0.14 and 0.46). Morphometric parameters of drainage networks include: Stream order (ranged between 4 and 5), Stream number (ranged between 44 and 1448), Stream lengths (ranged between 93.74 km and 3383.04 km), bifurcation ratio (ranged between 0.71 and 0.83), drainage density (ranged between 0.86km/km^2 and 1.13 km/km^2), Stream frequency (ranged between 0.40 strm/km and 0.50 strm/km) and drainage texture (ranged between 0.52 strm/km and 2.37 strm/km). Drainage basin relief parameters include: relief (ranged between 58m and 815m), mean slope (ranged between 2.55 deg. and 10.19 deg), slope aspect, relief ratio (ranged between 0.002 and 0.028), relative relief (ranged between 0.001 and 0.009), ruggedness number (ranged between 0.05 and 0.829), geometric number (ranged between 19.28 and 155.64) and Hypsometric integral (ranged between 0.17 and 4.08). The study concluded that the use of a digital elevation model based on GIS from ASTER DEM data is a more effective and successful method in the automatic extraction of morphometric parameters for drainage basins, integrated with topographic maps and satellite images. **[Bul. Soc. Géog. d'Égypte, 2020, 93: 131-158]**

Key Words: Automatic extraction, Watershed, GIS, DEM, Wadi Al-Adaira, KSA.

∗   Geography department, Faculty of Arts, Princess Noura Bint Abdul Rahman University, KSA.
∗∗ Geography department, College of Arts, King Saud University, KSA.
∗∗∗ College of Petroleum and Engineering & Geosciences, King Fahd University of Petroleum and Minerals, KSA.
    For Correspondence: e-mail: wsalkhuraiji@pnu.edu.sa

1. Introduction

Morphometric analysis of drainage networks is the primary basis for managing natural and hydrological resources, in addition to analyzing satellite imagery, topographic maps, and field survey, in this field automated extraction of the drainage network from DEMs received great attention (Al-Muqdadi & Merkel, 2011) (Chakrabortty, et al., 2018). The use of GIS technology in morphometric analysis is a powerful tool in many regions, especially in uninhabited areas (Bhunia, et al., 2012). In recent years, the use of watershed parameters through the use of GIS and DEM has increased more than manual techniques because of its high accuracy, flexibility, ease of storing maps, increasing their efficiency, and the ability to compare data and results with global research (Fattah & Yuce, 2015).

The digital elevation model (DEM) is a grid-based matrix structure, implicitly recording the relationships between the data points (Arun, et al., 2016), and is defined as a quantitative model of a part of the Earth's surface in digital form (Szypuła, 2017) (Reddy, et al., 2018). DEM data consists of either (1) a two-dimensional matrix of digital data representing the spatial distribution of heights on a regular network; (2) an digital data matrix for the x, y and z coordinates of an irregular grid of points; or (3) a digital data matrix stored in x, y shape along each contour line of a certain height (Walker & Willgoose, 1999).

In the last two decades, the morphometric parameters of drainage basins have been more common than the digital topography known as digital elevation models (DEM). The extraction of drainage networks play an important role in geomorphological analysis, hydrological modeling and provide a greater understanding of the variation of the prevailing geology, topographical information, tectonic structure of the basin and their interrelationships (Singh, et al., 2014). The topography of the drainage basins clearly affects the hydrological and geomorphological processes in the landscape. The spatial distribution of the terrain gives an indirect picture of the spatial change of these processes, using GIS techniques that store topographic data as raw data. DEMs are the basic data used for drainage terrain analysis, and digital elevation data analysis for hydrological and geomorphological applications. Some hydrological models using terrain digital representation (Moore, et al., 1991), and the information on drainage patterns, and topographic parameters can be obtained from the DEMs (Wu, et al., 2019).

DEM data can be captured from field survey using total station, GPS, topographic maps, or contour maps (Arun, et al., 2016), also from photogrammetry techniques (Walker & Willgoose, 1999), radar interferometry

and laser altimetry (Manuel, 2004), due to the difficulty of using these methods, their high costs and the unavailability of equipment, DEMs are provided through several open sources of satellites such as Asf. Vertex with a resolution of 12.5 m, Advanced Spaceborne Thermal Emission and Reflection Radiometer (ASTER) with a resolution of 30 m, the Shuttle Radar Topography Mission (SRTM) with a resolution of 90 m and 30 m (Singh, et al., 2014), or Cartosat-1 with a resolution of 30 m (Reddy, et al., 2018). The application of different automatic extraction methods on the same DEM data sources results in different results (Arun, 2013), and application of the same automatic extraction method to different DEM data also results in different results as the DEM resolution is a mean controller in the efficiency and accuracy of the terrain (Xen, et al., 2011).
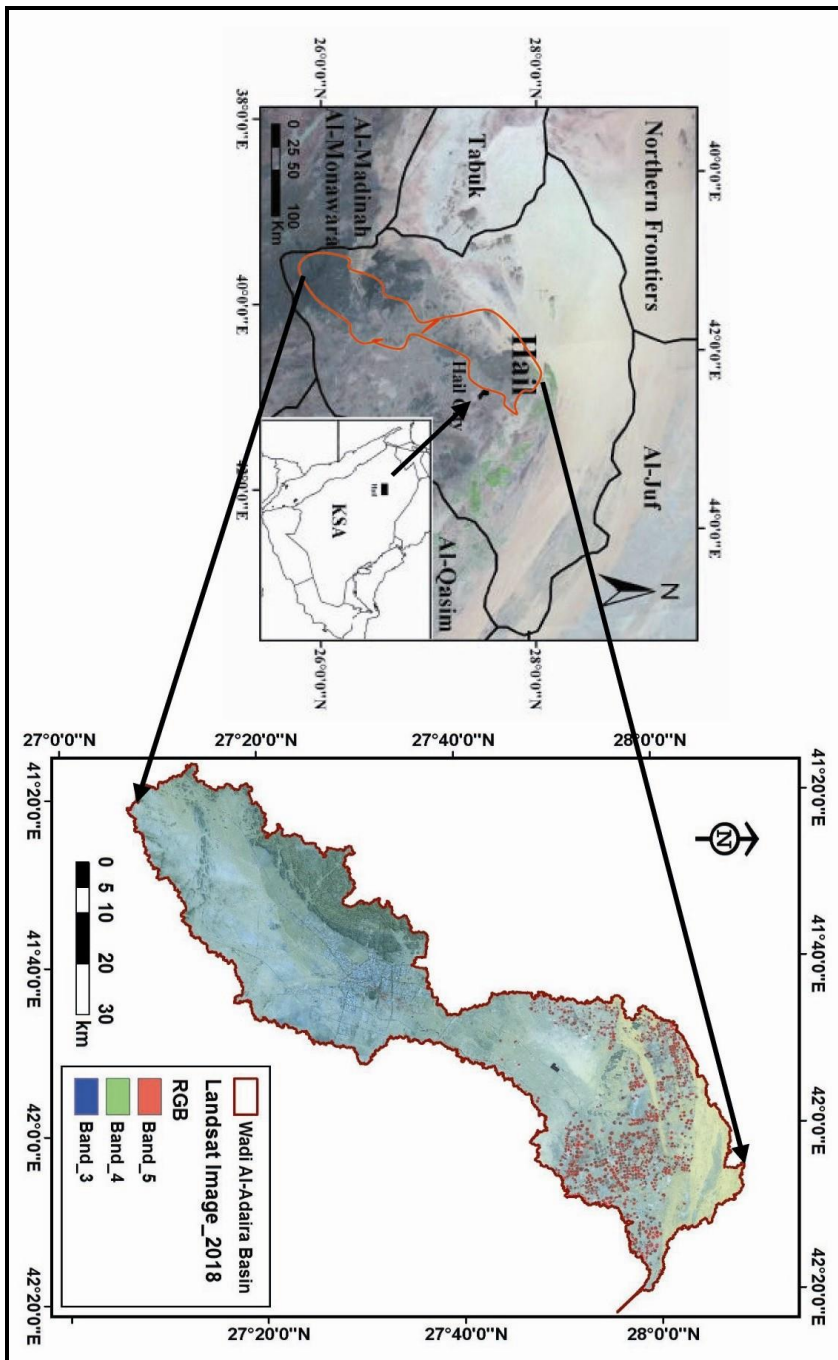
2.   Study Area
2.1 Location:

The Wadi Al-Adaira basin is one of the dry desert valleys located in the Hail province, north of the Najd plateau (north-central Saudi Arabia), between the latitudes 27° 06′ - 27° 52′ N., and between the longitudes 14° 16′ - 41° 59′ E. The basin extends from the southwest to the northeast with a length of 152.93 km (Figure 1), and limited to Jabal Aja (100 km long and 25-30 km wide) in northwest, and Jabal Salma (60 km long and 13 km wide) in southeast (El-Ghanim, et al., 2010). The area of the drainage basin is 5591.49 km^2.

2.2 Geological and Topographic Setting:

The study area is located within the Arabian Shield and the Great Nafud, associated with the Dahna, to the Empty Quarter in southern Arabia (Chapman, 1978). The mountainous zone of the study area consist of igneous and metamorphic rock that dates back to the pre-Cambrian period and represents the northern end of the Arabian Shield and is geologically defined by the Hail arch (Ekren, et al., 1986), The area of the Great Nafud is approximately 64,000 sq km, and it covers a large area of the Hail distric, which is a large depression dictated by sandy sediments derived from limestone rocks. (Abdel-Satar, et al., 2017). The main source of sand is the intrusive rocky granite block beneath the Arabian Shield, in addition, sand that appears in the form of sand dunes and sand sheets is partly derived from Paleozoic and Mesozoic sandstones formations (Chapman, 1978). The study area includes with different patterns of topography and land forms (Figure 2). The sand sheets covers the northern part of Hail, which is the second largest sand sea in the Arabian Peninsula, while rugged mountain ranges occupy the southern part, and geomorphological forms vary between them (Hereher, et al., 2012).
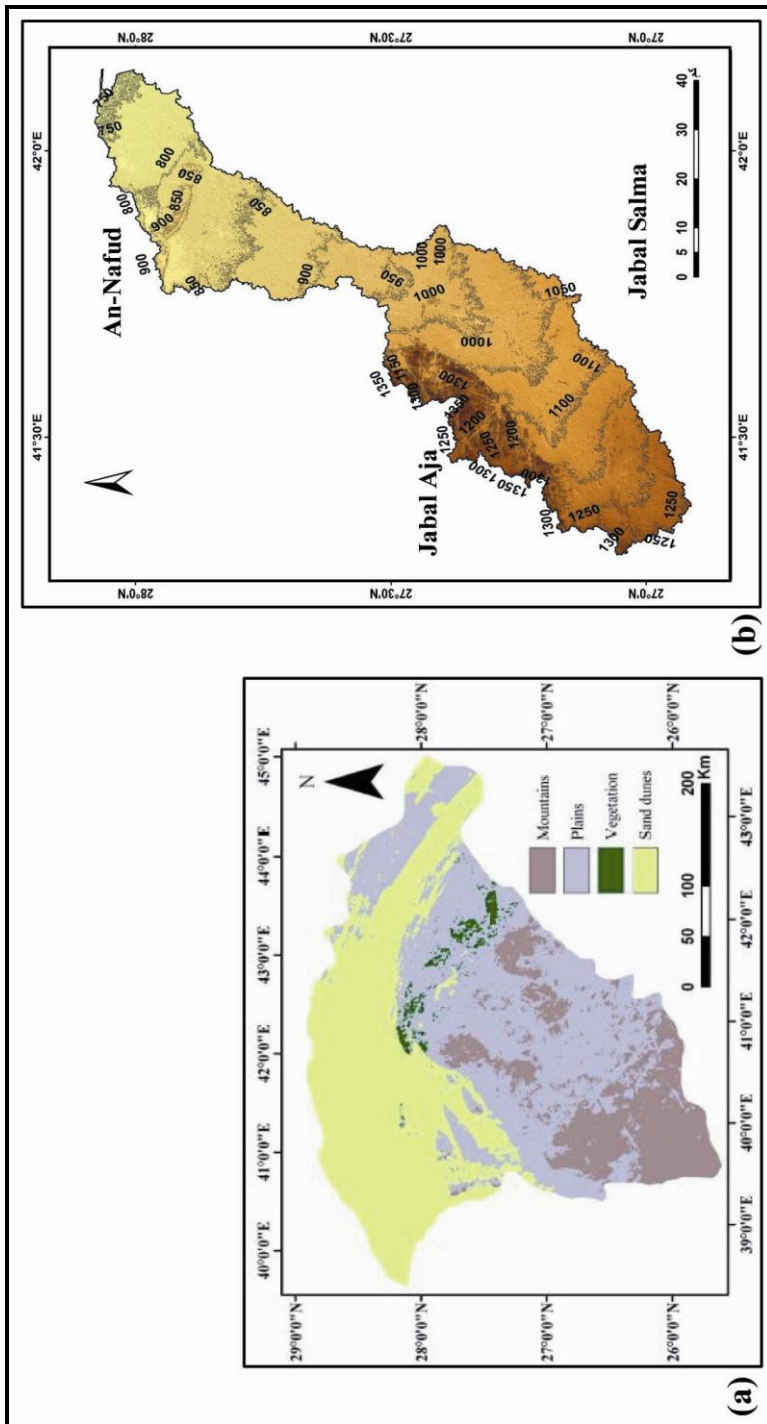
Figure 1. Location of Wadi Al-Adaira basin in Hail province.

Figure 2. (a) Land cover map of Hail District, after (Hereher et al., 2012). (**b**) Topographic characteristics of Wadi Al-Adaira Basin from (ASTER DEM data).

2.3 Climate Conditions:

The study area is characterized by the dominance of the continental desert climate, especially the cold winter and hot summer (Abdel-Satar, et al. 2017). Hail records showed from 2000 to 2018 that the average annual temperature is 25.6 °C, with an average maximum temperature of 34.1 °C in August, while the average minimum temperature is 10.8 °C in January. The annual precipitation is 104.4 mm, but it is characterized by irregularity, where the rain is concentrated in the winter and reaches in November (the about 32.0 mm/day), and there is no rainfall in the summer. On the other hand, the relative humidity is low in general, and its average annual rate is 31.0%. It decreases sharply in the summer and reaches 15.0% in July, but it increases relatively in winter, when it reaches January (53.0%). Wind in the study area with an average annual rate of 68.4 km/h, and the average number of stormy days is 25 annually. Due to the prevalence of the desert climate, the evaporation rate is generally low, ranging between 6.6 mm in December and 8.7 mm in August (El-Ghanim, et al., 2010).

3. Data and Methods
3.1 Data Sources:

This study used a multiple approach to multi-spectral, DEM sensed data and topographic sheets in Saudi Arabia to create a geodatabase and extract various morphometric parameters for Wadi Al-Adaira basin (Table 1).

3.1.1 Topographic and Geological Maps:

The topographic map included a scale of 1:50000 Hail sheet No. NG37-4, geological map scale 1:250000 Hail quadrangle No. 27E, geometrically and georeferenced maps were georeferenced through GCPs using UTM projection and WGS 84 datum, using Arc GIS, 10.5.

3.1.2 Satellite Images:

Included Landsat-8 Image ETM+ (2018) available on the USGS website.

Table 1. Data sources used in the study.

Type of data	Details of data	Sources
Topographic Map	scale: 1:50.000, Sheet NG37-4	Ministry of petroleum and mineral resources, KSA
Geological Map	Scale: 1:250.000, Sheet 27E	Ministry of petroleum and mineral resources, KSA
Landsat-8 Image	ETM+, row:041, path:169, Date16/8/2018	https://earthec\xplorer.usgs.gov
ASTER DEM, 30 m	ASTGTM2_N28E041_dem.tif	https://earthec\xplorer.usgs.gov
	ASTGTM2_N28E042_dem.tif	
	ASTGTM2_N27E041_dem.tif	
	ASTGTM2_N27E042_dem.tif	

3.1.3 Digital Elevation Model (DEM):

Was captured from ASTER DEM data with a resolution of 30 m, available on the USGS website. DEMs were produced from a combined project between the US NASA and Japan's Ministry of Economy, Trade and Industry (METI) (Szypuła, 2017). To prepare DEM data, Mosaic was integrated into the four DEMs covering the study area in a single raster layer using the Mosaic to new raters tool from Data Management tools in Arc GIS 10.5 and then converting the coordinate system of the raster layer from geographical coordinates (WGS 1984) to projected coordinates (UTM, zone 37 N) using Project Raster tool from Data Management tools. The study area was then cut from DEM to provide the time and effort required for the analysis using the Clip tool from Data Analysis tools. It was used in the preparation of the topographic characteristics, the slope and the mapping of the drainage network of the basin using the spatial analysis tool and Hydrology module Arc Hydro in Arc GIS 10.5 (Figure 3).

3.1.4 Morphometric parameters:

The ASTER DEM was automatically calculated using Arc GIS 10.5 and included the morphometric parameters of the drainage basin, the morphometric parameters of the drainage network, and the relief parameters, according to the morphometric parameters in Table (2).
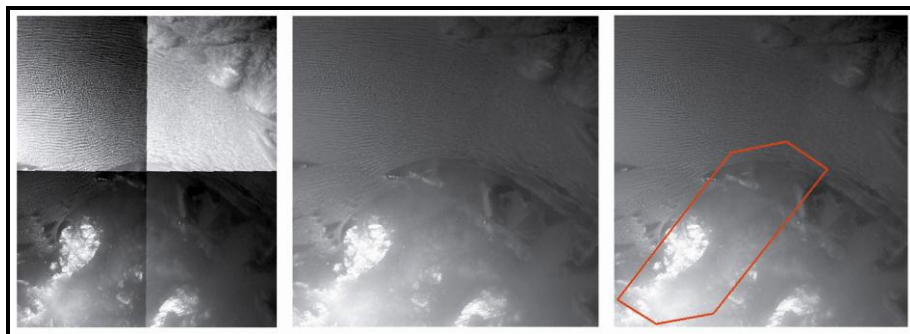

Figure 3. Mosaic and clip of study area from DEMs.

3.2 Methods:

A variety of methods have been developed for automated processing of raster data for DEMs for the extraction of drainage networks and their morphometric properties, i.e. O'Callaghan & Mark (1984); Wang & Liu (2006); Arun (2013); Ji & Qiuwen (2015); Liu, et al. (2017); Wu, et al. (2019); Rawat, et al. (2019).

Table 2. The methodology used to calculate of morphometric parameters.

Type	Parameters	Formula	References
Linear	Stream order (U)	Hierarchical rank	Strahler (1964)
	Stream number (Nu)	Number of the stream	Horton (1945)
	Stream length (Lu)	Total Length of stream (km)	Horton (1945)
	Bifurcation ratio (Rb)	Nu/(Nu+1)	Schumm (1956)
Areal	Area (A)	Area of the basin (km^2)	Strahler (1964)
	Max. basin length (Lb)	(km)	Gregory & Walling, (1976)
	Average basin width (W)	A/Lb (km)	Gregory & Walling, (1976)
	Basin perimeter (P)	Total length outer boundary of drainage basin (km)	Schumm (1956)
	Elongation ratio (ER)	$2\sqrt{A/\pi}/Lb$	Schumm (1956)
	Circulatory ratio (CR)	$4\pi A/P^2$	Miller (1953)
	Form factor (Rf)	A/Lb^2	Horton (1932)
	Drainage density (Dd)	Lu/A (km/km^2)	Horton (1932)
	Stream frequency (Fs)	Nu/A (strm/km^2)	Horton (1932)
	Drainage texture (Dt)	Nu/p (strm/km)	Horton (1945)
Relief	Basin relief (H)	Zmax-Zmin	Arc GIS
	Mean slope (Sm)	$\Delta E/L$	Eldaho (2002)
	Slope aspect	Automatic calculating	Arc GIS
	Relief ratio (Rh)	H//Lb (m/m)	Schumm (1956)
	Relative relief (Rr)	H/(P*100)	Strahler (1958)
	Ruggedness number (Rn)	H*D/1000	Strahler (1958)
	Geometric number (Gn)	R/Sb	Strahler (1958)
	Hypsometric integral (Hi)	A(km)/ H(m)	Gregory & Walling, (1976)

Extracting drainage networks from DEMs is based on the gravity; the water will flow from higher to lower elevation using the steepest descent and it is assumed that there is no interception, evapotranspiration and loss to groundwater. Automated extraction methods are the most efficient when DEM cell size is significantly smaller watershed dimensions (Ozdemir & Bird, 2009). The accuracy of the resulting terrain model depends on the dependent interpolation mechanism, which is based on the spatial autocorrelation principles, which assume that the nearest points are more similar than distant points. The literature reveals a great deal of interpolation

techniques that are generally classified into local and global methods (Watson, 1992) (Burrough and McDonnell, 1998) (Arun, 2013). However, studies in this direction have encountered some problems that restrict the benefits of these derivatives, such as errors during data collection, methodological errors and unknown errors, which are geographically due to different terrain conditions (Arun, et al., 2016), in addition to increasing data sizes due to increased accuracy, which makes the interpolation process very time consuming; in topographic depressions and flat areas, the resulting flow may sometimes be problematic in accurately representing the drainage patterns even if DEM is used from a higher resolution (Wu, et al., 2019), due to errors resulting from the interpolation of drainage networks such as lost cells values (gaps), Outliers, false sinks, false peaks and noise.

DEMs correction is an important process for hydrological analysis and modeling, such as the determination of flow directions and accumulations, and the delineation of drainage networks and sub-basins (Liu, et al., 2017). Enhancements in the efficiency and accuracy of DEMs lead to the production of more efficient drainage networks. The extraction of drainage networks from DEM was carried out using the Arc Hydro extension within Arc GIS (Liu & Zhang, 2010). Arc Hydro tools are based on the most widely used D8 algorithm (O'Callaghan & Mark, 1984). The main steps include: depression filling, flow direction determination, flow accumulation and stream definition (ESRI, 2005) (Figure 4).

3.2.1 Depression filling:

The fill and sinks operation, which removes the local depressions with an elevation value lower than all of its 8 neighbouring pixels and increases the pit to the lowest value of its 8 neighbour pixels (Koriche, 2012) (Figure 5). Hydrological analyzes have been initiated using the *Fill tool* to fill the gaps in the DEM layer and eliminate the Outliers values (higher or lower cell values than the average values of surrounding cells) from the *Hydrology* in *Spatial analysis tools*.

3.2.2 Flow direction determination:

Flow direction operation, which determines the direction of flow of water towards a neighbouring pixel having the steepest slope among the 8 neighbouring pixel (O'Callaghan, Mark, 1984) (Figure 6). The flow direction was calculated using the *Flow Direction tool* from *Hydrology* in *Spatial analysis tools*, it produces a raster layer containing the numbers: 1, 2, 4, 8, 16, 32, 64 and 128 which express the following flow direction respectively (East, South-East, South, South West, West, North West, North and North East) (Figure 7).
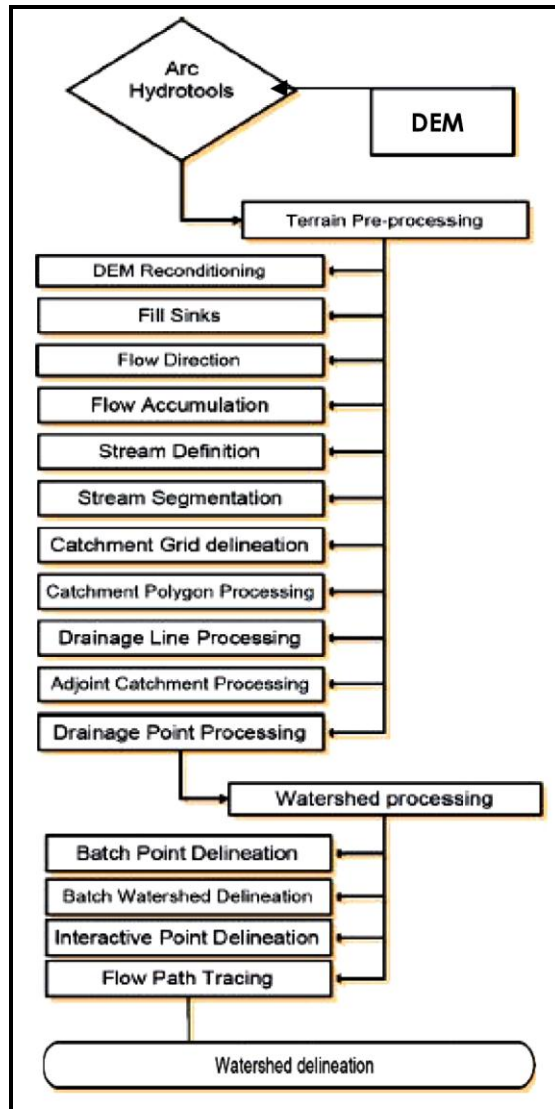
Figure 4. Flowchart for watershed extraction method,
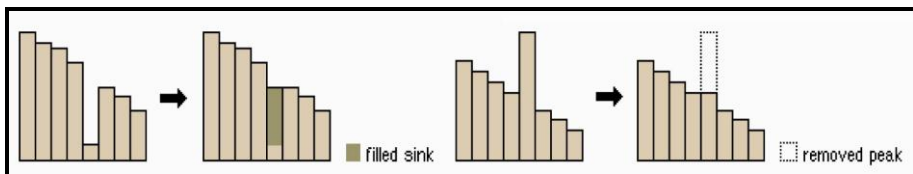after (Al-Muqdadi & Merkel, 2011).

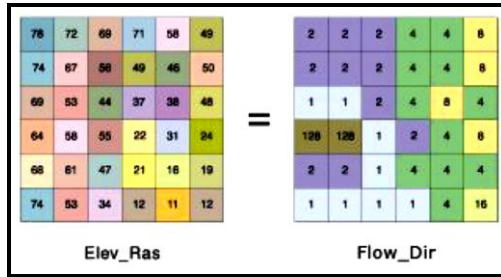**Figure 5.** Depression filling in GIS, after (ESRI, 2019).

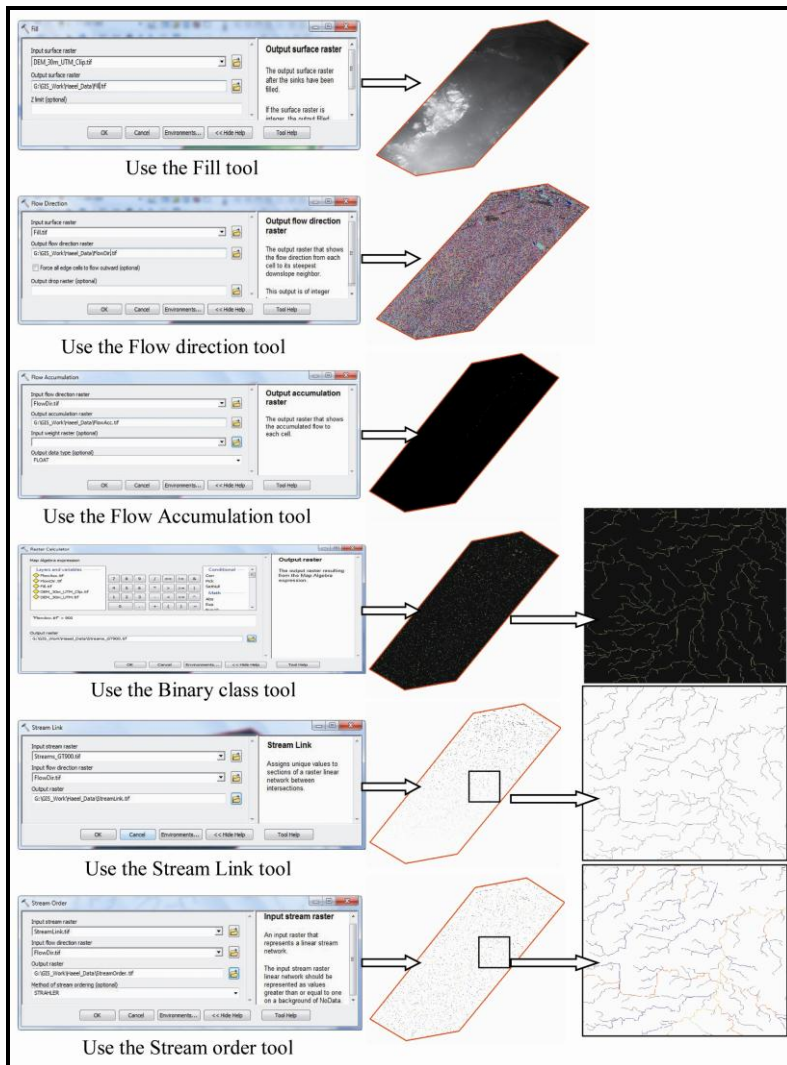**Figure 6.** Flow direction determination in GIS, after (ESRI, 2019).

Figure 7. Automated extraction of the drainage network of the Wadi Al-Adaira basin.

3.2.3 Flow accumulation:

The flow accumulation operation, which produce the number of upstream contributing pixels of a given outlet (Koriche, 2012) (Figure 8). The raster layer produces each cell at the highest number that expresses the number of cells above it and where the flow is calculated using the *Flow Accumulation tool* from *Hydrology* in *Spatial analysis tools*.

3.2.4 Stream Definition:

In this step, the cells in the previous layer (Flow Accumulation) with values greater than 900 streams were considered (this number can be reduced to increase the number of streams produced or greater than 900 to reduce the number of streams produced) Binary class (0 and 1), where cells of value 1 cross cells that were greater than 900 in the flow accumulation layer, which is defined as glaucoma, while zero cells represent cells less than 900 (Figure 9). The drainage network was determined using the *Raster Calculator tool* in *Spatial analysis tools*, then select the connection areas of the streams using the *Stream Link tool* from *Hydrology* in *Spatial analysis tools*, which assigns unique values to the linear network segments raster between intersections.
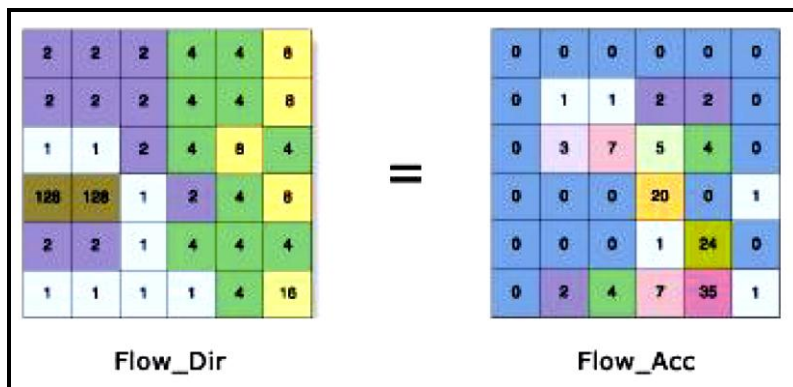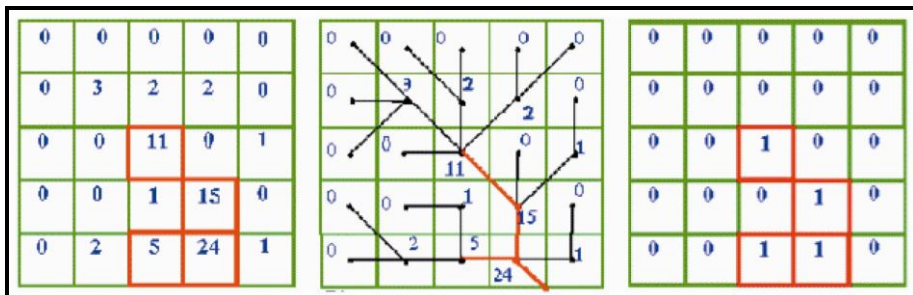

Figure 8. Flow accumulation in GIS, after (ESRI, 2019).

Figure 9. Stream definitions in GIS, after (ESRI, 2019).

3.2.5. Stream orders

Ordering systems are used to group or characterize the parts that constitute the drainage network. Horton (1945) proposed the first approach for channel ordering based on order concept. Later on, Strahler (1952) revised Horton's scheme and proposed some modification to avoid ambiguities, difficulties and restrictions related to subjective decisions (Afana, 2011). A top-down stream order system (also called Strahler Order) is used to classify stream segments based on the number of upstream tributaries (Radwan, et al., 2017).

With the Strahler system, stream order increases when streams of the same order intersect. For example, a second-order stream is formed by the junction of any of two first-order streams. The intersection of two streams of different orders will not increase the stream order (Strahler, 1952) (Figure 10) Stream ordering ranks the size and the flow regime of streams. It is a measure of the position of the stream in the tributary hierarchy and is sensitive to the accuracy of the drainage pattern delineation (Mourier, et al., 2008). Strahler method is sorted by using the *Stream Order tool* from *Hydrology* in *Spatial analysis tools* (Figure 11).

3.2.6. Sub-basins partition

Sub-basins are the distribution units of the natural distributor hydrologic model. The hydro processes within each sub-basin are carried out independently, reflecting in their entirety the spatial variation of the hydrological characteristics of the complete drainage basin. Arc GIS divides the drainage basins Sub-calculation of surface flow trends based on DEM data (Ji & Qiuwen, 2015) (Figure 12).
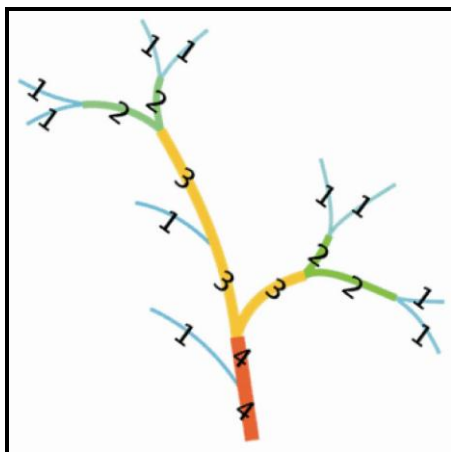

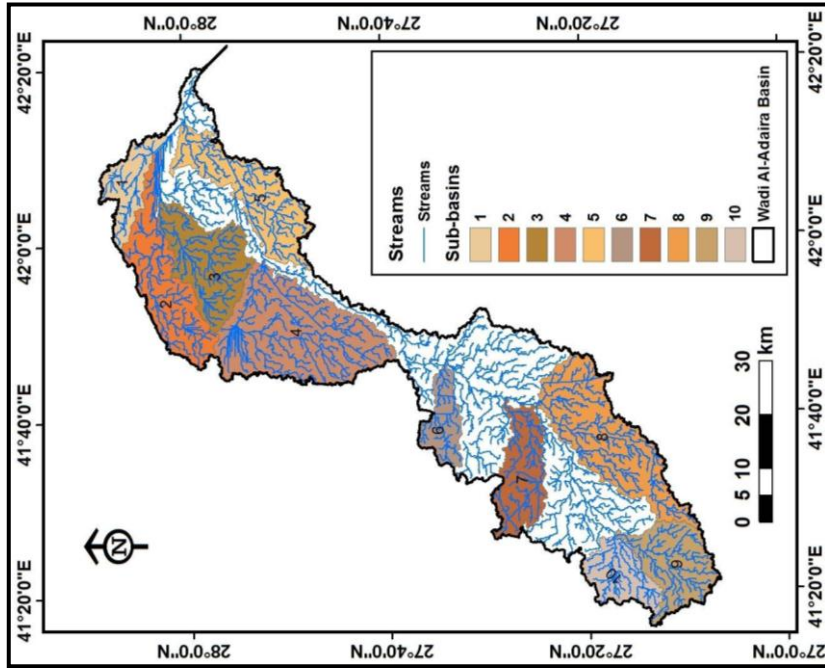**Figure 10.** Strahler Ordering System, modified after (Strahler, 1964).

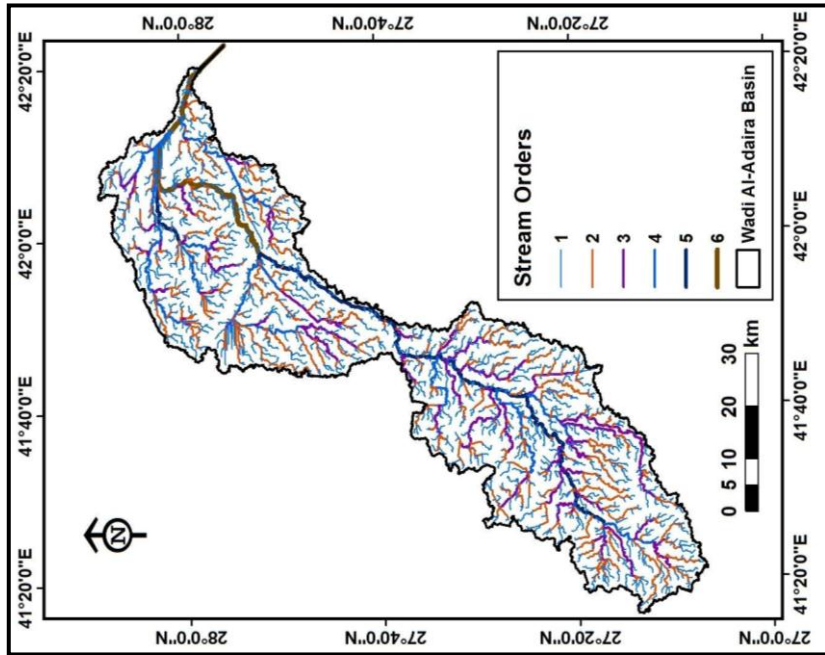**Figure 12.** Sub-basins of Wadi Al-Adaira basin.

Figure 11. Stream orders of Wadi Al-Adaira basin.

4.   Results and Discussion

Parameterization is defined as the numerical description of the continuous surface form (Pike, 2000) and is geomorphologically defined as a set of measurements that describe the topography sufficiently well to distinguish the topographical aspects of the topography (Ehsani, 2008).

4.1 The morphometric parameters of drainage basins:

The morphometric parameters of drainage basins included: area (A), Max. length (Lb), average width (W), perimeter (P), elongation ratio (ER), circulation ratio (CR) and form factor (Ff) (Table 3).

Table 3. Morphometric parameters of drainage basins.

Basin	A (km^2)	Lb (km)	W (km)	P (km)	ER	CR	Ff
1	109.57	24.32	4.51	84.48	0.49	0.19	0.19
2	258.03	41.62	6.20	133.36	0.44	0.18	0.15
3	231.93	26.98	8.60	107.89	0.64	0.25	0.32
4	471.68	31.93	14.77	144.84	0.77	0.28	0.46
5	254.94	36.64	6.96	142.28	0.49	0.16	0.19
6	92.50	19.25	4.81	62.45	0.56	0.30	0.25
7	172.32	28.33	6.08	102.38	0.52	0.21	0.21
8	362.96	38.54	9.42	152.67	0.56	0.20	0.24
9	190.09	21.91	8.68	97.18	0.71	0.25	0.40
10	124.41	17.06	7.29	69.56	0.74	0.32	0.43
11	3323.06	152.93	21.73	610.03	0.43	0.11	0.14

A Basin area, *Lb* Max. Basin length, *W* Average basin width, *p* Basin perimeter, *ER* Elongation ratio, *CR* circulation ratio, *Ff* Form factor.

4.1.1. Basin area (A):

The area of the sub-basins ranged between 92.5 km^2 (basin No. 6) and 3323.06 km^2 (basin No. 11). The average area was 508.32 km^2.

4.1.2. Basin length (Lb):

Represents the straight line connecting the mouth of the basin and the farthest point on the basin's perimeter. Length of the sub-basins ranged between 17.06 km (basin No. 10) and 152.93 km (basin No.11). The average area was 39.95 km.

4.1.3. Basin width (W):

The width of the sub-basins ranged between 4.51 km (basin No.1) and 21.73 km (basin No.11). The average area was 9.00 km.

4.1.4. Basin perimeter (P):

Represents the actual length of the water divided line that separates the study drainage basin and the other drainage basins adjacent to it. Perimeter of the sub-basins ranged between 62.45 km (basin No. 6) and 610.03 km (basin No. 11). The average area was 155.19 km.

4.1.5. Elongation ratio (ER):

Is the ratio between the diameter of a circle of the same area as the drainage watershed and the maximum length of the watershed (Schumm, 1956). Elongation ratio of the sub-basins ranged between 0.43 (basin No. 11) and 0.77 (basin No. 4). The average area was 0.57. The elongation ratio indicates a decrease in the bifurcation rate, which leads to delayed surface runoff, low risk of flash floods, and an increase in the recharge of groundwater aquifers, this is evident in the basin No. 1, 2 and 11.

4.1.6. Circulation Ratio (CR):

Is the ratio of the area of the watershed to the area of a circle having the same circumference as the perimeter of the watershed (Miller, 1953; Strahler, 1964). Circularity ratio of the sub-basins ranged between 0.11 (basin No.11) and 0.32 (basin No. 10). The average area was 0.22. The lower circulation ratio indicates an increase in the bifurcation rate, which enhances runoff, and increases the risk of flash floods, this is evident in the basin No. 6 and 10.

4.1.7. Form Factor (Ff):

Horton (1932) expressed the shape of the watershed as form factor and defined it as a dimensional ratio of the area to the watershed length. Form factor of the sub-basins ranged between 0.14 (basin No. 11) and 0.46 (basin No. 4). The average area was 0.27. The low form factor indicates the inconsistency of the shape of the drainage basins due to the geological structure controlled, this is evident in the basin No. 1, 2, 5 and 11.

4.2 The morphometric parameters of the drainage networks:

The morphometric parameters of the drainage networks included: stream order (U), stream number (Nu), stream lengths (SL), bifurcation ratio (BR), drainage density (Dd), stream frequency (SF) and drainage texture (Dt) (Table 4).

Table 4. Morphometric parameters of the drainage networks.

Basin	U	Nu	SL (km)	BR	Dd (km/km²)	Dt (strm/km)	SF (strm/km)
1	4	44.00	93.74	0.76	0.86	0.52	0.40
2	4	123.00	269.13	0.82	1.04	0.92	0.48
3	5	108.00	241.00	0.74	1.04	1.00	0.47
4	5	200.00	477.11	0.77	1.01	1.38	0.42
5	4	105.00	250.83	0.81	0.98	0.74	0.41
6	4	46.00	97.03	0.76	1.05	0.74	0.50
7	5	81.00	173.44	0.71	1.01	0.79	0.47
8	4	152.00	374.59	0.83	1.03	1.00	0.42
9	4	78.00	193.45	0.80	1.02	0.80	0.41
10	4	62.00	140.61	0.78	1.13	0.89	0.50
11	6	1448.00	3382.04	0.80	1.02	2.37	0.44

U Stream order, *Nu* Stream number, *SL* Stream length, *BR* Bifurcation ratio, *Dd* Drainage density, *Dt* Drainage texture, *SF* Stream frequency.

4.2.1 Stream order (U):

The main stream order rank for the drainage basin was 6 (VI). The stream order of the sub-basins ranged between 4 (basins No.1, 2, 5, 6, 8, 9 and 10) and 5 (basins No. 3, 4 and 7).

4.2.2 Stream number (Nu):

The total number of streams reached 2447 stream. Stream number of the sub-basins ranged between 44 (basin No.1) and 1448 (basin No.11) (Figure 13). The average area was 222.

4.2.3 Stream length (SL):

Based on Horton's law Horton (1945), consequently, the stream length has been measured from the basin mouth to the drainage divide (Kant, et al. 2015). Stream length of the sub-basins ranged between 93.74 km (basin No. 1) and 3383.04 km (basin No. 11) (Figure 14). The average area was 517.54 km. The stream length is one of the most significant hydrological features of the watershed as it can be considered as a proxy for the surface runoff characteristics (Radwan, et al., 2017), where it is inversely proportional to the risk of flash floods because of the increased losses of evaporation and infiltration, this is evident in the basin No. 4 and 11.

4.2.4 Bifurcation ratio (BR):

Represents the ratio between the stream number relative to a certain order and the stream number relative to the next higher order, is found according to (Schumm, 1956). Bifurcation ratio of the sub-basins ranged between 0.71 (basin No.7) and 0.83 (basin No. 8). The average area was 0.78. The lower bifurcation ratio increases the amount of surface runoff that reaches the downstream and thus increases the risk of flash floods, this is evident in the basin No. 1, 3, 4, 6 and 7.
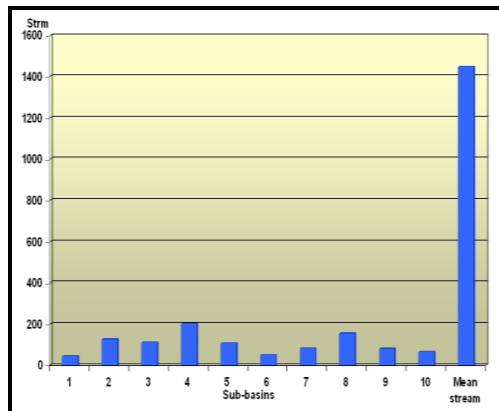

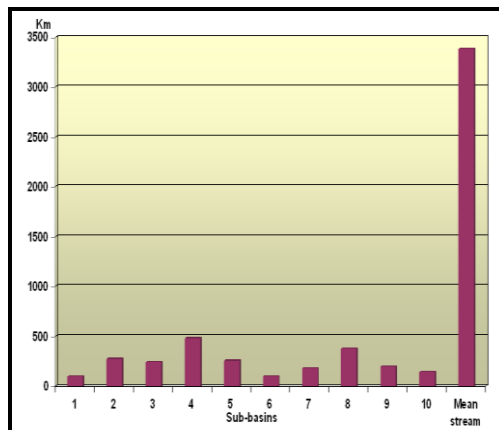**Figure 13.** Stream numbers of the sub-basins.

Figure 14. Stream lengths of the sub-basins.

4.2.5 Drainage density (Dd):

Is a measure to analyze the length of different streams per unit area, and it is obtained by dividing the total stream length by the total watershed area (Horton, 1932). Drainage density of the sub-basins ranged between 0.86 km/km^2 (basin No. 1) and 1.13 km/km^2 (basin No. 10). The average area

was 1.01 km/km². High drainage density is related to the increase in the amount of surface runoff, especially in watersheds which high in stream frequency and low in the bifurcation ratio, this is evident in the basin No. 10.

4.2.6 Drainage texture (Dt):

This term refers to the length of the run off of the rain water on the ground surface before it gets concentrated into definite stream channels. This factor relates inversely to the average slope of the channel and is quite synonymous with the length of sheet flow to large degrees (Chakrabortty et al., 2018). Drainage texture of the sub-basins ranged between 0.52 strm/km (basin No. 1) and 2.37 strm/km (basin No. 11). The average area was 1.01 strm/km. Thus, in the watersheds they are located within the fine Drainage texture, which is characterized by poor vegetation and low rain, especially in basin No. 1.

4.2.7 Stream frequency (SF):

Is the number of stream segments per unit area (Horton, 1945). It is obtained by dividing the total number of streams by the total watershed area. Stream frequency of the sub-basins ranged between 0.40 strm/km (basin No. 1) and 0.50 strm/km (basins No. 6 and 10). The average area was 0.44 strm/km. High stream frequency is related to the increase in the amount of surface runoff and thus an increased risk of flash floods, this is evident in the basin No. 6 and 10.

4.3 The relief parameters of drainage basins:

The relief parameters of drainage basins included: elevation (H), mean slope (Ms), slope aspect (Sa), relief ratio (Rr), relative relief (RR), ruggedness number (Rn), geometric number (Gn) and hypsometric integral (Hi) (Table 5).

Table 5. The relief parameters of drainage basins.

Basin	H (m)	Ms (deg.)	Rr	RR	Rn	Gn	Hi
1	58.00	2.55	0.002	0.001	0.050	20.80	1.89
2	240.00	3.05	0.006	0.002	0.250	43.41	1.08
3	252.00	3.51	0.009	0.002	0.262	28.03	0.92
4	187.00	3.08	0.006	0.001	0.189	32.30	2.52
5	139.00	3.19	0.004	0.001	0.137	36.05	1.83
6	535.00	9.40	0.028	0.009	0.561	20.19	0.17
7	504.00	10.19	0.018	0.005	0.507	28.51	0.34
8	263.00	3.92	0.007	0.002	0.271	39.77	1.38
9	290.00	4.37	0.013	0.003	0.295	22.30	0.66
10	361.00	6.50	0.021	0.005	0.408	19.28	0.34
11	815.00	4.53	0.005	0.001	0.829	155.64	4.08

H Basin relief, *Ms* Mean slope, *Rr* Relief ratio, *RR* Relative relief, *Rn* Ruggedness number, *Gn* Geometric number, *Hi* Hypsometric integral.

4.3.1 Elevation:

Notice the variation of elevation of Wadi Al-Adaira Basin, where the elevation (< 800 m) is the largest percentage of the area of 26.76%, followed by the elevation (800-900 m), where occupies area 20.11%, then those tow categories cover the area of 46.87%. The lowest percentage of the area is covered by elevation (> 1200 m) where occupies area (12.09%) (Table 6 and Figure 15).

Table 6. Elevation categories of drainage basin.

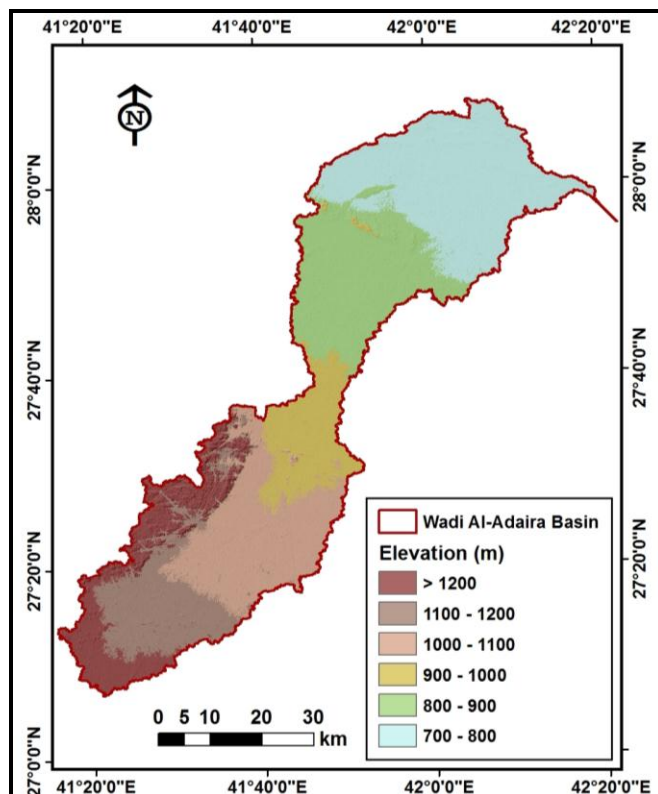| Elevation (m)	Area (km^2)	%
<800	889.12	26.76
800-900	668.35	20.11
900-1000	336.99	10.14
1000-1100	602.24	18.12
1100-1200	424.71	12.78
>1200	401.62	12.09
Total	3323.02	100.00

Figure 15. Elevation categories of Wadi Al-Adaira basin.

-150-

4.3.2 Basin Relief (H):

Represents the difference between the maximum elevation and the lowest elevation within the watershed. Relief is an important attribute of terrain in general and the drainage watershed in particular. The relief measures are indicative of the potential energy of the drainage system because of its elevation above the mean sea level (Sakthivel et al., 2019). Basin relief of the sub-basins ranged between 58 m (basin No. 1) and 815 m (basin No. 11). The average area was 331.27 m.

4.3.3 Slope (S):

Represents the loss or gain in altitude per horizontal distance in a direction (Bhunia, et al., 2012). The slopes that range from 2-5 degree cover a higher percentage of the study area of 36.97%, followed by the slope that range > 2 degree, where cover 34.28%, then those tow categories cover the area of 71.25%. The lowest percentage of the area is covered by slope greater than 45 degree (0.02%) (Table 7 and Figure 16). Slope the most important and specific feature of the earth's surface forms (Chakrabortty, et al., 2018).

4.3.4 Mean slope (Ms):

Watershed slope reflects the rate of change of elevation with respect to distance along the principal flow path. $\Delta S = E/L$; where ΔE is difference in elevation (between the end points of the principal flow path); L is hydrologic length of the flow path (Eldaho, 2002). The mean slope of the sub-basins ranged between 2.55 deg. (basin No. 1) and 10.19 deg. (basin No. 7). The average area was 4.93 deg. The increase in slope leads to an increase in the speed of the surface runoff and a decrease in the infiltration rate, thus increasing the risk of flash floods, this is evident in the basin No. 6 and 7.

Table 7. Slope categories of drainage basin.

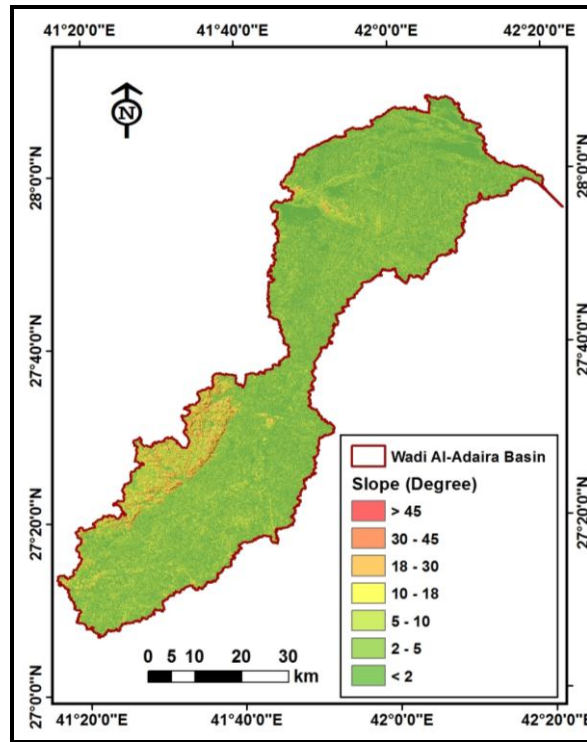| Slope (Deg.)	Area (km^2)	%
< 2	1139.07	34.28
2-5	1228.64	36.97
5-10	652.40	19.63
10-18	178.68	5.38
18-30	95.74	2.88
30-45	27.73	0.83
> 45	0.77	0.02
Total	**3323.02**	**100.00**

Figure 16. Slope categories of Wadi Al-Adaira basin.

4.3.5 Slope aspects (Sa):

North-oriented slope covers the largest area of the study area (24.45%), followed by southwest-oriented slope (12.63%), and Northeast-oriented slope (12.39%) (Figure 17 and Table 8).

Table 8. Aspects categories of drainage basin.

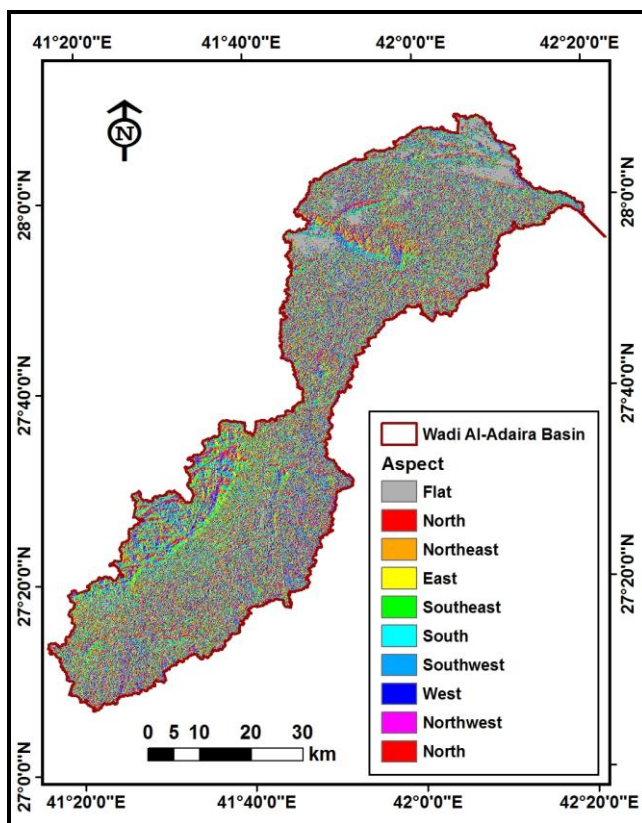| Slope (Deg.)	Area (km^2)	%
Level	227.86	6.86
North	812.53	24.45
Northeast	411.75	12.39
East	362.58	10.91
South	394.41	11.87
Southwest	419.65	12.63
West	373.20	11.23
Northwest	321.04	9.66
Total	**3323.02**	**100.00**

Figure 17. Aspects categories of Wadi Al-Adaira basin.

4.3.6. Relief ratio (Rr):

When watershed relief is divided by the horizontal distance on which it is measured, it results in a dimensionless relief ratio (Schumn, 1954). It measures the overall steepness of a drainage watershed and is an indicator of the intensity of erosion process (Sakthivel, et al., 2019). Relief ratio of the sub-basins ranged between 0.002 (basin No. 1) and 0.028 (basin No. 6). The average area was 0.01.

4.3.7. Relative relief (RR):

The relative relief (RR) represents actual variation of altitude in a unit area with respect to its local base level. The RR does not take into account the dynamic potential of the terrain but as it is closely associated with slopes. It is defined as the difference in height between the highest and the lowest points in 100 km^2 grid areas (Bhunia, et al., 2012). Relative relief of the sub-basins ranged between 0.001 (basins No. 1, 4, 5 and 11) and 0.009 (basin No. 6). The average area was 0.003.

4.3.8. Ruggedness number (Rn):

Is the product of drainage density and basin relief (Strahler, 1958) in the same unit. Ruggedness number of the sub-basins ranged between 0.05 (basin No. 1) and 0.829 (basin No. 11). The average area was 0.341. The low of ruggedness number leads to a decrease in the drainage density in the basins due to its small area, this is evident in the basin No. 1, 4 and 5.

4.3.9. Geometric number (Gn):

The sub-basins ranged between 19.28 (basin No.10) and 155.64 (basin No.11). The average area was 40.57.

4.3.10 Hypsometric integral (Hi):

To develop relationship between horizontal cross-sectional area of watershed and elevation (Eldaho, 2002). Hypsometric integral of the sub-basins ranged between 0.17 (basin No.6) and 4.08 (basin No.11). The average area was 1.38. High values of Hypsometric integral indicate an increase in the basins area versus lower relief, indicating the long period of time that the basins during its geomorphological cycle, this is evident in the basin No. 4 and 11.

5.   Conclusion

The present study used the GIS-based digital elevation model (DEM) in automatic extraction of the morphometric parameters of the Wadi Al-Adaira basin in Saudi Arabia. The results of the study showed that the length of the watershed was increased in relation to its width and therefore tends to elongation and decreased Circulation, which leads to delayed arrival of runoff from the upper stream to the downstream mouth near Hail City. The basins is also characterized by a decrease in the values of relief and roughness because of the large area of the basin for the extent of the relief. As a result, the study concluded that the use of GIS-based digital elevation model from ASTER DEM data is a more effective, successful and accurate method of automatic extraction of morphometric parameters of drainage basins.

Acknowledgment

References

1. Abdel-Satar, AM., Al-Khabbas, M.H., Alahmad, W.R., Yousef, W.M., Alsomadi, R.H., Iqbal, T., (2017) Quality assessment of groundwater and agricultural soil in Hail region, Saudi Arabia. Egypt J. of Aquatic Res., 43(1): 55-64.

2. Afana, A., (2011): Delineation of channel networks from Digital Elevation Models (DEMs). Ph.D. the University of America, 387p.

3. Al-Muqdadi, M.W. & Merkel, B.J., (2011): Automated watershed evaluation of flat terrain. Journal of Water Resource and Protection, 3: 892-903.

4. Arun, P.V., (2013): A comparative analysis of different DEM interpolation methods. Egypt J. Remote Sens. Space Sci., 16: 133–139.

5. Arun, P.V., Katiyar, S.K., Prasad, V., (2016): Performances evaluation of different open source DEM using differential global positioning system (DGPS). Egypt J. Remote Sens. Space Sci., 19: 7–16.

6. Bhunia, G.S., Samanta, S., Pal, B. (2012): Quantitative analysis of relief characteristics using space technology. International Journal of Physical and Social Sciences, 2(8): 350-365.

7. Burrough, P.A., McDonnell, R.A., (1998) :Principles of geographical information systems. Oxford University Press, New York, pp.333–335.

8. Chakrabortty, R., Ghosh, S., Chandra, S., Das, B., Malik, S., 2018. Morphometric Analysis for hydrological assessment using remote sensing and GIS technique: A case study of Dwarkeswar River basin of bankura district, west Bengal. Asian Journal of Research in Social Sciences and Humanities, 8(4): 113-142.

9. Chapman, R.W., 1978. Geomorphology. In: Al-Sayari, S.S., Zotl, J.G. (Eds.), Quaternary period in Saudi Arabia. Springer-Verlag Inc., NY, :19–30.

10. Ehsani, A.H., (2008): Morphometric and landscape feature analysis with artificial neural networks and SRTM data applications in humid and arid environments. Ph.D. Royal Institute of Technology, Stockholm, Sweden. 71p.

11. Ekren, E.B., Vaslet, D., Berthiaux, A., Strat, P.L., Fourniguet, J., (1986) :Explanatory notes to the geology map of the Hail quadrangle, Sheet 27E, Kingdom of Saudi Arabia, Ministry of petroleum and mineral resources, 46p.

12. Eldaho, T.I., (2002): Watershed modeling. IIT Bombay, https://nptel.ac.in/courses.

13. El-Ghanim, W.M., Hassan, L.M., Galal, T.M., Badr, A., (2010) :Floristic composition and vegetation analysis in Hail region north of central Saudi Arabia. Saudi Journal of Biological Sciences, 17: 119–128.

14. ESRI. (2005): Arc Hydro tools - tutorial. Environmental Systems Research Institute, Redland, CA, USA, 112p.

15. ESRI. (2019): A Tool reference. https://pro.arcgis.com

16. Fattah, W.H. & Yuce, M.I., 2015. Hydrological Analysis of Murat River basin. International Journal of Applied Science and Technology, 5(5): 47-55.

17. Gregory, K.J. & Walling, D.E. (1976): Drainage Basin Form and Process A Geomorphological Approach, Edward Arnold, London, 458p

18. Hereher, M.E., Al-Shammari, A.M., Abd Allah, S.E., (2012): Land cover classification of Hail, Saudi Arabia using remote sensing. International Journal of Geosciences, 3: 349-356.

19. Horton, R.E., (1932): Drainage-basin characteristics Eos. Trans. Am. Geophys. Union, 13: 350–361.

20. Horton, R.E., (1945): Erosional development of stream and their drainage basins; hydrological approach to quantitative morphology. Geological Society of America Bulletin, 56(3): 275-370.

21. Ji, S. & Qiuwen, Z., (2015): A GIS-based subcatchments division approach for SWMM. The Open Civil Engineering Journal. 9: 515-521.

22. Kant, S., Meshram, S., Dohare, R., Singh, S., (2015): Morphometric analysis of Sonar sub-basin using SRTM data and geographical information system (GIS). Afr. J. Agric. Res., 10: 1401–1406.

23. Koriche, S.A., (2012): Remote sensing based hydrological modelling for flood early warning in the upper and middle Awash river basin. Master Deg. Faculty of Geo-Information Science and Earth Observation of the University of Twente. 58p.

24. Liu, X. & Zhang, Z., (2010): Extracting drainage network from high resolution DEM in Toowoomba, Queensland. In: Queensland surveying and spatial conference, 1-3 Sept, Brisbane, Australia.

25. Liu, X., Wang, N., Shao, J., Chu, X., (2017): An automated processing algorithm for flat areas resulting from DEM filling and interpolation. Int. J. Geo-Inf. 6: 1-14.

26. Manuel, P., (2004): Influence of DEM interpolation methods in drainage analysis. GIS Hydro., 4: 1-26.

27. Miller, V.C., (1953): A quantitative geomorphic study of drainage basin characteristics in the Clinch Mountain area Virginia and Tennessee. Columbia Univ., New York.

28. Moore, I.D., Grayson, R.B., Ladson, A.R., (1991): Digital terrain modelling: a review of hydrological, geomorphological and biological applications. Hydrol. Process, 5: 3–30.

29. Mourier, B., Walter, C., Merot, P., (2008): Soil distribution in valleys according to stream order. Catena, 72: 395-404.

30. O'Callaghan, J.F., Mark, D.M., (1984): The extraction of drainage networks from digital elevation data. Comput. Vision Graph. Image Process. 28: 323-344.

31. Ozdemir, H. & Bird, D., (2009): Evaluation of morphometric parameters of drainage networks derived from topographic maps and DEM in point of floods. Environ. Geol., 56: 1405–1415.

32. Pike, R.J., (2000): Geomorphology diversity in quantitative surface analysis. Progress in Physical Geography, 24: 1-20.

33. Radwan, F., Alazba., A.A., Mossad, A., (2017): Watershed morphometric analysis of Wadi Baish Dam catchment area using integrated GIS-based approach. Arab J Geosci., 10(256): 1-11.

34. Rawat, K.S., Singh, S.K., Singh, M.I., Garg, B.L., (2019): Comparative evaluation of vertical accuracy of elevated points with ground control points from ASTER DEM and SRTM DEM with respect to CARTOSAT-1 DEM. Egypt J. Remote Sens. Space Sci. 13: 289–297.

35. Reddy, G., Kumar, N., Sahu, N., Singh, S., (2018): Evaluation of automatic drainage extraction thresholds using ASTER GDEM and Cartosat-1 DEM: A case study from basaltic terrain of Central India, Egypt J. Remote Sens. Space Sci. 21: 95-104.

36. Sakthivel, R., Raj, N., Sivasankar, V., Akhila, P., Omine, K., (2019): Geo-spatial technique-based approach on drainage morphometric analysis at Kalrayan Hills, Tamil Nadu, India. Applied Water Science, 9(24): 1-18.

37. Schumm, S.A., (1956): Evolution of drainage systems and slopes in badlands at Perth Amboy, New Jersey. Geol. Soc. Am. Bull., 67: 597–646.

38. Singh, P., Gupta, A., Singh, M., (2014): Hydrological inferences from watershed analysis for water resource management using remote sensing and GIS techniques. Egypt J. Remote Sens. Space Sci. 17: 111–121.

39. Strahler, A.N. (1958): Dimensional analysis applied to fluvially eroded landforms, Bull. Geol. Soc. America, 69: 279-300.

40. Strahler, A.N., (1952): Hypsometric (area-altitude) analysis of erosional topography. Geological Society of America Bulletin. 63(11): 1117-1142.

41. Strahler, A.N., (1964):. Quantitative geomorphology of drainage basin and channel networks. Handbook of applied hydrology. McGraw-Hill, New York.

42. Szypuła, B. (2017): Digital elevation models in geomorphology. digital elevation models in geomorphology. In: Shukla, D.P. (Eds.), Hydro-Geomorphology Models and Trends. INTECH: 81-112.

43. Walker, J.P., Willgoose, G.R., (1999): On the effect of digital elevation model accuracy on hydrology and geomorphology. Water Resources Research, 35(7): 2259–2268.

44. Wang, L., Liu, H., (2006): An efficient method for identifying and filling surface depressions in digital elevation models for hydrologic analysis and modelling. Int. J. Geogr. Inf. Sci. 20: 193–213.

45. Watson, D., (1992):Contouring: A guide to the analysis and display of Spatial data. pergamon Press, London, pp.120–123

46. Wu, T., Li, J., Li, T., Sivakumar, B., Zhang, G., Wang., (2019): High-efficient extraction of drainage networks from digital elevation models constrained by enhanced flow enforcement from known river maps. Geomorphology. 340: 184–201.

الملخص العربى

هدفت الدراسة إلى تقييم إمكانية استخدام نموذج الارتفاع الرقمي (DEM) بالاعتماد على تقنية نظـم المعلومـات الجغرافيـة فـي الاستخراج الآلـي لشبكة حـوض التصـريف وحسـاب معاملاتهـا المورفومترية. واستخدمت الدراسة نموذج الارتفاع الرقمي من بيانات (ASTER DEM 30 m) لحوض وادي الأديرع وأحواضه الفرعية باستخدام برنامج Arc GIS 10.5 وملحقاته المتمثلة في: أدوات التحليل المكاني وأدوات التحليل ثلاثي الأبعاد والتحليل الهيدرولوجي، ثم حساب المعاملات المورفومترية لأحواض التصريف، والتي شملت: المساحة (تتراوح بين ٩٢.٥ كم٢ و ٣٣٢٣.٠٦ كم٢)، وأقصى طول حوضي (تراوح بين ١٧.٠٦ كم و ١٥٢.٩٣ كم) ، ومتوسط العرض (تراوح بين ٤.٥١ كم و ٢١.٧٣ كم)، والمحيط (تراوح بين ٦٢.٤٥ كم و ٦١٠.٠٣ كم)، ونسبة الاستطالة (تراوحت بين ٠.٤٣ و ٠.٧٧)، ونسبة الاستدارة (تراوحت بين ٠.١١ و ٠.٣٢)، ومعامل الشكل (تراوح بين ٠.١٤ و ٠.٤٦). وتضمنت المعاملات المورفومترية لشبكات التصريف: ترتيب المجاري (تراوحت بين ٤ و ٥)، وأعداد المجاري (تراوحت بين ٤٤ و ١٤٤٨)، وأطوال المجاري (تراوحت بين ٩٣.٧٤ كم و ٣٣٨٣.٠٤ كم) ، ونسبة التفرع (تراوحت بين ٠.٧١ و ٠.٨٣)، وكثافة التصريف (تراوحت بين ٠.٨٦ كم/كم٢ و ١.١٣ كم/كم٢)، وتكرار المجاري (تراوح بين ٠.٤٠ درجـة/كم و ٠.٥٠ دورة/كم) ونسيج التصريف (تراوح بين ٠.٥٢ درجة / كم و ٢.٣٧ مسار / كم)، وتضمنت المعاملات التضاريسية لأحواض التصريف: التضاريس (تراوحت بين ٥٨ م و ٨١٥ م)، ومتوسط الانحدار (تراوح بين ٢.٥٥ درجة و ١٠.١٩ درجة)، واتجاه الانحدار، ونسبة التضرس (تراوحت بين ٠.٠٠٢ و ٠.٠٢٨)، والتضاريس النسبية (تراوحت بين ٠.٠٠١ و ٠.٠٠٩)، ودرجة الوعورة (تراوح بين ٠.٠٠٥ و ٠.٨٢٩)، والرقم الجيومتري (تراوح بين ١٩.٢٨ و ١٥٥.٦٤) والتكامل الهبسومتري (تراوح بين ٠.١٧ و ٤.٠٨). وخلصت الدراسة إلى أن استخدام نموذج الارتفاع الرقمي المعتمد على نظم المعلومات الجغرافية من بيانات ASTER DEM يعد طريقة فاعلة وناجحة في الاستخراج الآلـي للمعـاملات المورفومتريـة لأحـواض التصـريف بالتكامـل مـع الخـرائط الطبوغرافيـة وصـور الأقمـار الصناعية.